

STRUCTURE AND PROPERTIES OF MD SIMULATED $\text{Na}_2\text{O} \cdot \text{SiO}_2$ MELT COMPARISON OF THE BORN-MAYER-HUGGINS AND PAULING INTERIONIC POTENTIALS

BEATA HATALOVÁ, MAREK LIŠKA

Institute of Inorganic Chemistry of the Slovak Academy of Sciences, Dúbravská cesta 9, 842 36 Bratislava

Received 5. 2. 1992.

MD simulations of $\text{Na}_2\text{O} \cdot \text{SiO}_2$ melt were performed using Born-Mayer-Huggins and Pauling pair potential functions in the temperature range of 1000–2000 K. Thermodynamic properties as total energy, pressure and heat capacity were compared for the two simulated systems as well as their structural characteristics. Thermodynamic behaviour of both systems is similar and the calculated values of the heat capacity are close to the experimental one. There are some differences between the simulated structures: Born-Mayer-Huggins pair potential functions support occurrence of some silicon atoms coordinated by five oxygens and more branched structure of silicate polyanions with many rather small rings. On the other hand, the structure simulated using Pauling pair potential functions has more chain-like character with few large rings and there are no 5-coordinated silicon atoms present.

INTRODUCTION

In recent years the method of molecular dynamics (MD) has been widely used to elucidate the random structure of silica and silicate melts and glasses as well as some of their properties [14,15]. All these simulations are based on ionic approximation and two types of interionic potentials have been mostly applied, the Born-Mayer-Huggins potential (BMH) parametrized by Woodcock [1] and the Pauling potential (PA) parametrized by Mitra [2]. All parameters were adjusted to fit the properties of SiO_2 and both potentials do work well enough to reproduce the local tetrahedral network structure of amorphous silica. Some problems occur when alkalis are added to SiO_2 and become more obvious with increasing concentration of alkali oxide. They concern the presence of 5-coordinated silicon atoms and increasing of pressure in simulated systems.

Different authors reported the results for alkali silicates [3,4,16–19] but always using only one of the mentioned potentials. Comparison of these results is rather difficult because not only the content of alkali oxides was different, but the cooling procedures varied seriously, as well.

The aim of this work is to show the differences in simulated $\text{Na}_2\text{O} \cdot \text{SiO}_2$ structure and properties using BMH and PA pair potential functions (PPFs) with parameters that were employed in simulations of sodium silicate systems by Soules [3] and Mitra [4], respectively.

METHOD

The system of 378 particles (63 Si, 189 O and 126 Na) was simulated applying periodic boundary conditions. The density of the system was kept constant. It was obtained by linear extrapolation from experimental data [5] for temperature 1873 K, that is

2.11 g/cm³. Simulations were performed for two models of interionic interactions; the first represented by BMH PPFs

$$V_{ij} = A_{ij} \exp\left(\frac{-r_{ij}}{\rho}\right) + \frac{z_i z_j e^2}{4\pi\epsilon_0 r_{ij}} \quad (1)$$

$$A_{ij} = (1 + z_i/v_i + z_j/v_j) b \exp\left(\frac{\sigma_i + \sigma_j}{\rho}\right) \quad (2)$$

and the second by PA PPFs defined as interparticle force:

$$F_{ij} = \frac{z_i z_j e^2 r_{ij}}{4\pi\epsilon_0 r_{ij}^3} \left[1 + \text{sign}(z_i z_j) \left(\frac{\sigma_i + \sigma_j}{r_{ij}}\right)^n \right] \quad (3)$$

where r_{ij} is the distance between the i -th and j -th particles, z the electronic charge, σ the ionic radius, v the number of valence shell electrons, b and ρ are constants and n is the measure of the repulsion force. Parameters of the individual ion pairs [3,4] are summarized in Table I.

The simulations started from a random configuration at 5000 K. After 2000 time steps (2ps) the system was cooled down to 3000, then 2500 and 2000 K by scaling the velocities of all particles. Each decrease of temperature was followed by 2ps long equilibration. From 2000 to 1000 K the cooling procedure comprised sudden decrease of the temperature by 100 K followed by 1ps equilibration (with numeric control of the set temperature) and another 1 μ s of measuring phase.

Individual simulation runs were carried out to obtain results for comparison with X-ray diffraction experiment [6] at 1873, 1673 and 1523 K. They started from the configurations reached in the previous simulations for the closest temperature and employed the same cooling procedure except the temperature was set to the required values.

All calculations were performed using the P3M3DP program [7] that comprises the calculation of total Coulomb force by particle-particle particle-mesh

Table I

Parameters of the used pair potential functions

Potential type	Parameter	Si	O	Na
Born-Mayer -Huggins	z_i	+4	-2	+1
	σ_i [Å]	1.15	1.42	1.17
	v_i	8	8	8
	b [J] e [Å]	3.38×10^{-20} 0.29		
Pauling	z_i	+2.272	-1.136	+0.568
	σ_i [Å]	0.2374	1.2	0.823
	n	10		

method [8]. The numerical integration time step was 10^{-15} s.

RESULTS AND DISCUSSION

Thermodynamic properties

As it is obvious from the values of ionic charges the total energy of the system simulated with BMH PPFs is about 2.8 times greater than with PA PPFs. Using the linear least squares method the values of isochoric

heat capacity c_V and thermal pressure coefficient γ_V were calculated from the temperature dependences of total energy and pressure of the simulated systems, respectively. These are shown in Figs. 1 and 2.

The isobaric heat capacity c_p of the simulated systems was calculated according to the following equation

$$c_p = c_V + \alpha_p \gamma_V T \quad (4)$$

where c_V and γ_V were taken from the simulation results (as mentioned above), the thermal expansivity α_p was calculated from the density measurements [5], and temperature 1500 K was taken as the mean value of the temperature interval 1000–2000 K for which c_V was determined. The results and comparison with experiment are shown in Table II.

The calculation of pressure from the virial theorem is not accurate enough, so in MD simulations the pressure up to 0.5 GPa is considered the normal pressure [2]. In both simulated systems the pressure was higher. It ranged from 0.8 to 3 GPa. As it has been shown in other works, pressure would lower if the density of simulated system was lowered. For example, MD study of the molar volume of $\text{Na}_2\text{O} \cdot 3\text{SiO}_2$ using BMH PPFs for description of interparticle interactions [9] gave the molar volume about $22 \text{ cm}^3/\text{mol}$ for the melt at 2000 K. That is the density of 1.57 g/cm^3 only, comparing with the value 2.165 g/cm^3 extrapolated from the density measurements [10]. Similar problems with the density of sodium trisilicate were reported by Murray et al. who used combined Keat-

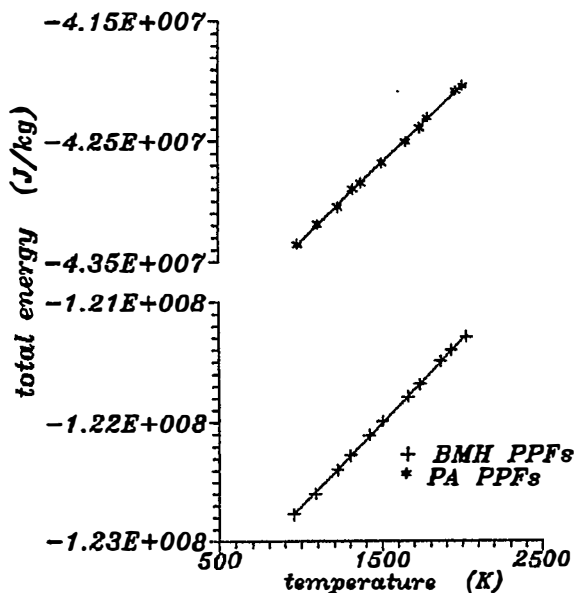


Fig. 1. Temperature dependence of the total energy in $\text{Na}_2\text{O} \cdot \text{SiO}_2$ melt simulated using Born-Mayer-Huggins (BMH) and Pauling (PA) pair potential functions (PPFs).

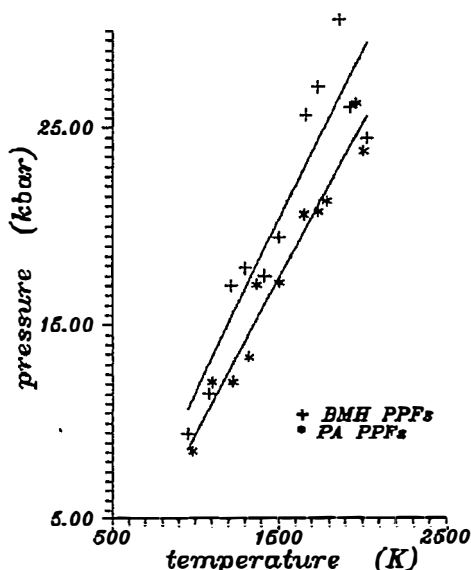


Fig. 2. Temperature dependence of the pressure in $\text{Na}_2\text{O} \cdot \text{SiO}_2$ melt simulated using Born-Mayer-Huggins (BMH) and Pauling (PA) pair potential functions (PPFs).

Table II

Calculated and experimental values of the thermal pressure coefficient γ_V , thermal expansivity coefficient α_p , isochoric and isobaric heat capacity c_V and c_p , respectively

Potential type	γ_V [MPa K ⁻¹]	α_p [m ³ kg ⁻¹ K ⁻¹]	c_V [J kg ⁻¹ K ⁻¹]	c_p [J kg ⁻¹ K ⁻¹]
BMH	1.74	–	1399.4	1519
PA	1.58	–	1301.0	1409
Experiment	–	4.57×10^{-8} *	–	1454**

*Ref. [5]

**Ref. [6]

ing and Lenard-Jones potential [11] for modelling its structure. Such high pressure was not observed in cases when SiO_2 was simulated in accordance with the small thermal expansivity of silica. Application of the potential functions parametrized for SiO_2 to alkali silicate systems may lead to mentioned increase of pressure, as well.

Despite the high pressure in the simulated systems the values of the heat capacity and thermal pressure coefficient are reasonable comparing with experiment.

Structure

The main features of the structure of simulated $\text{Na}_2\text{O} \cdot \text{SiO}_2$ melt for both types of PPFs are similar. In

agreement with general opinion the structure is built of SiO_4 tetrahedra that are connected through their corners. The tetrahedra are only slightly distorted, as the mean OSiO bond angle is close to the value for regular tetrahedron – 109.47°. The mean values and distributions of the SiOSi bond angle for both simulated systems reflexing the arrangement of tetrahedra are in Table IV and Fig. 6, as well as the results for intertetrahedral bond angle OSiO. Sodium ions are placed in intermediate sites of the silicate framework. Their coordination sphere created by oxygens is not regular and the number of neighbouring oxygens vary.

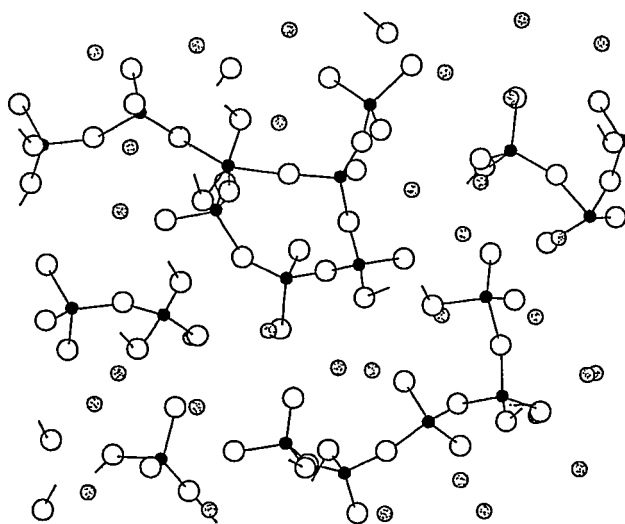


Fig. 3. The structure of $\text{Na}_2\text{O} \cdot \text{SiO}_2$ melt simulated using BMH PPFs at 1673 K.

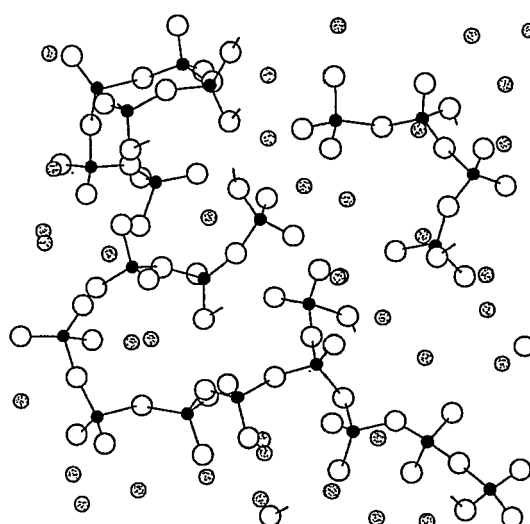


Fig. 4. The structure of $\text{Na}_2\text{O} \cdot \text{SiO}_2$ melt simulated using PA PPFs at 1673 K.

Table III

Temperature dependence of the parameters of short range order, average distance r_{ij} [10^{-10} m] and coordination number N_{ij} , in molten $\text{Na}_2\text{O}\cdot\text{SiO}_2$ and its MD models simulated using Born-Mayer-Huggins (BMH) and Pauling (PA) potential functions

	T [K]	SiO		NaO		O O		Si Si	
		r_{ij}	N_{ij}	r_{ij}	N_{ij}	r_{ij}	N_{ij}	r_{ij}	N_{ij}
BMH	1873	1.65	4.06	2.25	2.7	2.67	4.1	3.29	2.2
	1673	1.65	4.05	2.28	2.7	2.65	4.1	3.29	2.2
	1523	1.65	4.04	2.23	2.5	2.64	4.2	3.29	2.2
PA	1873	1.62	4.00	2.19	3.4	2.60	4.1	3.17	2.1
	1673	1.62	4.00	2.22	3.3	2.60	4.1	3.16	2.1
	1523	1.62	4.00	2.21	3.3	2.59	4.1	3.14	2.1
Exp. [6]	1873	1.61	3.8	2.32	5.4	2.66	5.6	3.24	2.9
	1673	1.61	3.9	2.34	5.5	2.65	5.8	3.22	3.1
	1523	1.62	3.8	2.35	5.7	2.66	5.9	3.20	3.4

Comparison of the short range structure characteristics, i.e. bond lengths and coordination numbers, with X-ray diffraction experiment [6] is presented in Table III. The bond lengths represented by positions of the first maxima in the pair radial distribution functions (RDFs) agree quite well for all pairs.

Significant differences between the simulations and experiment occurred in coordination numbers. Though the experimental error for coordination numbers is 0.3, the differences for OO and SiSi pairs are much bigger. The values for the MD modeled melts are by 0.7–1.8 lower than those determined from the X-ray measurement. However, from the theoretical point of view $\text{Na}_2\text{O}\cdot\text{SiO}_2$ is built of tetrahedra with two bridging and two non-bridging oxygens that are connected into chains. That is the structure of crystalline sodium silicate, as well, and this chain-like structure supports the coordination number SiSi equal 2 rather than 2.9–3.4 from the diffraction results (Table III). The ^{29}Si NMR measurements of sodium silicate glass support this value, too, because only tetrahedra with two bridging oxygens were observed [12]. The most distinct differences in the coordination number for NaO pairs can be explained by the character of NaO pair RDF (Fig. 5). The coordination sphere of Na ion is not well defined, so it is difficult to set the cut-off distance for its first coordination sphere. If the cut-off distance is set to the first flat minimum after first maximum in the NaO RDF (these results), the coordination number comprises perhaps only the non-bridging oxygen neighbours.

The short range order parameters are constant in the studied temperature interval (Table III).

Comparison of the structures simulated using BMH and PA PPFs yields the following results:

1) BMH PPFs support occurrence of some silicon atoms that are coordinated by 5 oxygens. This can be identified by rising of the mean coordination number over the value of 4 (Table III), as well as in the OSiO bond angle distribution function (Fig. 6). A small shoulder appears at the lower angle side of the main peak together with a very small and flat peak at 150° – 180° . They represent the angles in a deformed trigonal bipyramid which arises from a coordination tetrahedron when the fifth oxygen enters coordination sphere of a silicon atom [13]. The presence of

Table IV

The mean bond angles for the simulated structure at 1673 K. The numbers in brackets are the standard deviations

Potential type	Bond angle [$^\circ$]			
	OSiO		SiOSi	
BMH	109.1	(10.2)	156.7	(11.2)
PA	109.2	(7.7)	150.7	(13.6)

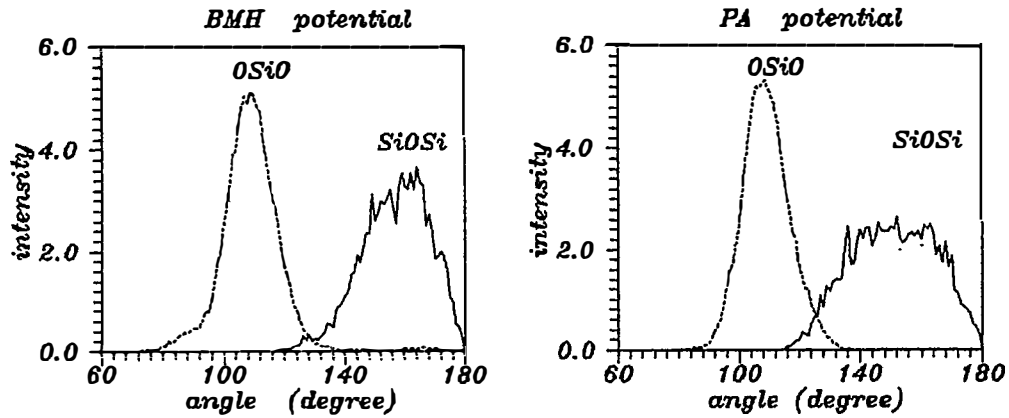


Fig. 6. Bond angle distributions of the simulated $\text{Na}_2\text{O} \cdot \text{SiO}_2$ melts.

Table V

Percentage of species in the simulated melts at 1673 K

Potential type	Coordination species					
	Ω_0	Ω_1	Ω_2	Ω_3	Ω_4	Ω_5
BMH	3.17	19.05	44.44	26.98	1.58	4.76
PA	1.59	14.29	61.90	17.46	4.76	—

5-coordination might be the result of inadequate ratio of the anion/cation radii, that is 1.23 for BMH parametrization, though it should be at least 2.44 [20].

2) The two structures differ in the bridging to non-bridging oxygen ratio and in the distribution of Ω_n species that represent tetrahedra with n bridging oxygens [12]. The species Ω_5 , present in the structure simulated using BMH PPFs, is the case of a 5-coordinated silicon with all bridging oxygens. While the theoretical value of the bridging to non-bridging oxygen ratio for $\text{Na}_2\text{O} \cdot \text{SiO}_2$ is 0.5, we obtained 0.59 and 0.55 for BMH and PA PPFs, respectively. The distribution of Ω_n species is in Table V, and shows, that the structure obtained using BMH PPFs is more branched than the other one. It consists of many smaller rings including 4–6 tetrahedra while the structure obtained using PA PPFs has more chain-like character with small number of large rings with 8 to 15 tetrahedra. Comparing these facts with ^{29}Si NMR results [12] that confirm only presence of Ω_2 species and admit less than 10% of the others, the structure obtained using PA PPFs seems more realistic.

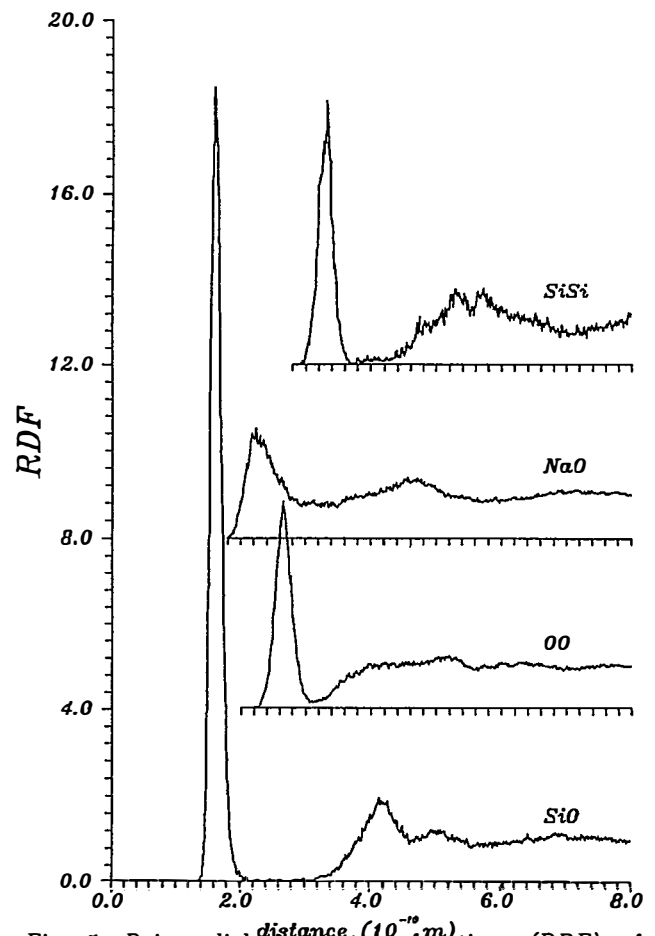


Fig. 5. Pair radial distribution functions (RDF) of $\text{Na}_2\text{O} \cdot \text{SiO}_2$ melt simulated using BMH PPFs at 1673 K.

CONCLUSIONS

The MD models of sodium silicate melt obtained using Born-Mayer-Huggins and Pauling PPFs [3,4] for description of interparticle interactions agree in the main features rather well with experimental findings, though there are some differences between both simulated structures. Thermodynamic properties of the systems, except the total energy, are similar for both potential types and their parametrizations. The heat capacities and thermal pressure coefficients have reasonable values, but the pressure is quite high.

The first step to improvement of MD results should be reparametrization of the present PPFs because their parameters, as in general all fitted ones, may depend on chemical composition of a simulated system.

References

- [1] Woodcock L. V., Angell C. A., Cheeseman P.: *J. Chem. Phys.* **65**, 1565 (1976).
- [2] Mitra S. K.: *Phil. Mag.* **B45**, 529 (1982).
- [3] Soules T. F.: *J. Chem. Phys.* **71**, 4570 (1979).
- [4] Mitra S. K., Hockney R. W. in: *The Structure of Non-Crystalline Materials*, (ed. by Gaskell P. H., Parker, J. M.), p. 316, Taylor and Francis Ltd., New York 1983.
- [5] Coenen M. in: *Svojstva Stekol i Stekloobrazujushtchich Rasplavov I.*, (ed. by Mazurin O. V., Strelcina M. V., Schvajko-Schvajkovskaja T. P.), p. 210, Nauka, Leningrad 1973.
- [6] Waseda Y., Toguri J. M.: *Transactions ISIJ* **17**, 601 (1977).
- [7] Eastwood J. W., Hockney R. W., Lawrence D. N.: *Computer Phys. Commun.* **19**, 215 (1980).
- [8] Eastwood J. W. in: *Computational Methods in Classical and Quantum Physics* (ed. by Hooper M. B.), p. 206, Advance Publications, London 1976.
- [9] Soules T. F.: *J. Non-Cryst. Solids* **49**, 29 (1982).
- [10] Heidtkamp G., Endell K. in: *Svojstva Stekol i Stekloobrazujushtchich Rasplavov I.*, (ed. by Mazurin O. V., Strelcina M. V., Schvajko-Schvajkovskaja T. P.), p. 204, Nauka, Leningrad 1973.
- [11] Murray R. A., Song L. W., Ching W. Y.: *J. Non-Cryst. Solids* **94**, 133 (1987).
- [12] Dupree R., Holland D., McMillan P. W., Pettifer R. F.: *J. Non-Cryst. Solids* **68**, 399 (1984).
- [13] Hatalová B., Liška M.: *J. Non-Cryst. Solids* **146**, 218 (1992).
- [14] Soules T. F. in: *Glass, Science and Technology*, Vol. 4A, Structure, Microstructure and Properties, (ed. by Uhlman D. R., Kreidl N. J.), p. 267, Academic Press, New York, 1990.
- [15] Hatalová B., Liška M.: *Ceramics-Silikáty* **32**, 359 (1988).
- [16] Angel C. A., Cheeseman P. A., Tamaddon S.: *Science* **218**, 885 (1982).
- [17] Tesar A. A., Varshneya A. K.: *J. Chem. Phys.* **87**, 2986 (1987).
- [18] Newell R. G., Feuston B. P., Garofalini S. H.: *J. Mater. Res.* **4**, 434 (1989).
- [19] Inoue H., Yasui I.: *Phys. Chem. Glasses* **28**, 63 (1987).
- [20] Dekker A. J.: *Solid State Physics*, p. 127, Prentice-Hall, Englewood Cliffs 1957.

Submitted in English by the authors

MD MODEL TAVENINY $\text{Na}_2\text{O} \cdot \text{SiO}_2$.
POROVNANIE BORN-MAYER-HUGGINSOVÝCH
A PAULINGOVÝCH INTERAKČNÝCH POTENCIÁLOV

BEATA HATALOVÁ, MAREK LIŠKA

Ústav anorganickej chémie SAV,
Dúbravská cesta 9, 842 36 Bratislava

V teplotnom intervale 1000 – 2000 K bola metódou molekulovej dynamiky simulovaná tavenina $\text{Na}_2\text{O} \cdot \text{SiO}_2$. V jednom súbore boli medzičasticové sily reprezentované Born-Mayer-Hugginsovými (BMH) a v druhom Paulingovými (PA) párovými potenciálovými funkciami. Odhliadnuc od celkovej energie, ktorá je v dôsledku vysokých nábojov v prípade BMH potenciálov 2.8-krát väčšia, sú termodynamické vlastnosti oboch súborov veľmi podobné. V oboch je príliš vysoký tlak, čo však nemá vplyv na hodnoty izochorickej teplotnej rozpínavosti a merného tepla. Napriek dobrej zhode oboch štruktúr s výsledkami röntgenovej difrakčnej analýzy, navzájom sa v detailoch odlišujú. BMH potenciálové funkcie vedú k rozvetvenej štruktúre s veľkým počtom pomerne malých cyklov vytvorených tetraédrami SiO_4 , v ktorej sa však nachádzajú aj atómy kremíka koordinované piatimi kyslíkmi. Štruktúra, ktorá vzniká pri simulácii s použitím PA potenciálových funkcií, je charakterizovaná reťazcami prepojenými len do niekoľkých veľkých cyklov a všetky atómy kremíka sa nachádzajú v tetraedrickej koordinácii kyslíkom.

Obr. 1. Teplotná závislosť celkovej energie v simulovaných systémoch $\text{Na}_2\text{O} \cdot \text{SiO}_2$ s použitím Born-Mayer-Hugginsových (BMH) a Paulingových (PA) párových potenciálových funkcií (PPFs).

Obr. 2. Teplotná závislosť tlaku v simulovaných systémoch $\text{Na}_2\text{O} \cdot \text{SiO}_2$ s použitím BMH a PA PPFs.

Obr. 3. Štruktúra taveniny $\text{Na}_2\text{O} \cdot \text{SiO}_2$ simulovanej s použitím BMH PPFs pri teplote 1673 K.

Obr. 4. Štruktúra taveniny $\text{Na}_2\text{O} \cdot \text{SiO}_2$ simulovanej s použitím PA PPFs pri teplote 1673 K.

Obr. 5. Párové radiálne distribučné funkcie pre taveninu $\text{Na}_2\text{O} \cdot \text{SiO}_2$ simulovanú s použitím BMH PPFs pri 1673 K.

Obr. 6. Distribúcie väzbových uhlov v simulovanej tavenine $\text{Na}_2\text{O} \cdot \text{SiO}_2$.